J. Cent. South Univ. (2018) 25: 331−341
DOI: https://doi.org/10.1007/s11771-018-3740-9

Springer

Effect of geometric micro-groove texture patterns on tribological performance of stainless steel

CHEN Ping(陈平), LI Jun-ling(李俊玲), LI Yun-long(李云龙)

School of Mechanical Engineering, University of Science and Technology Beijing, Beijing 100083, China

Abstract: This work describes an experimental investigation into the influence of geometric micro-groove texture patterns on the tribological performance of stainless steel. Five geometries were studied: one with untextured and four with micro-groove textured making parallel, triangular, square and hexagonal patterns. The micro-groove textures were produced using an MFT-20 laser system as well as a two-step laser surface texturing (LST) process. Tribological performance was measured using a pin-on-disk tribometer. The investigation showed that the two-step LST process could fabricate high-precision micro-grooves. The experimental data indicated that the micro-groove textured surfaces achieved the lower frictional coefficients than the untextured surface and the geometric patterns had significantly affected the tribological properties of samples in both lubricated and unlubricated states. The results were analyzed from the lubricant supplying and fluid dynamic pressure effect under lubricated conditions as well as abrasive capture and remove under dry friction conditions.

Key words: geometric pattern; micro-groove texture; frictional coefficient

Cite this article as: CHEN Ping, LI Jun-ling, LI Yun-long. Effect of geometric micro-groove texture patterns on tribological performance of stainless steel [J]. Journal of Central South University, 2018, 25(2): 331–341. DOI: https://doi.org/10.1007/s11771-018-3740-9.

1 Introduction

Great efforts to reduce friction and wear are very important for increasing efficiency and durability of mechanical parts. Significant developments in advanced materials and innovative methods to increase the tribological properties of friction pairs are expected as a result of on-going research in the area of engineering [1–3]. The surface pattern technology has demonstrated its high potential to reduce loss from friction and wear. Surface texture technology therefore is emerging as an effective method to enhance the tribological performance of mechanical components [4–6]. As early as 1966, a report by HAMILTON et al [7] displayed a patterned surface with micro-asperities and showed that under the lubricated state the micro-asperities acted as micro hydrodynamic bearings. In recent decades, surface texture technology has been successfully used in various fields to increase the tribological performance of friction surfaces. Prominent examples are golf balls, hard disks, mechanical seals, engine cylinders and sliding bearings [4, 8, 9]. Improvements due to surface texturing have been widely reported in applications ranging from dry friction [6], boundary lubrication [10] to hydrodynamic lubrication [11] because artificial patterns can capture wear particles to reduce further abrasion wear [12, 13], act as micro-reservoirs to retain the lubricant [14, 15] and produce additional fluid dynamic pressure to

Foundation item: Project(51305023) supported by the National Natural Science Foundation of China; Project(FRF-GF-17-B20) supported by the Fundamental Research Funds for the Central Universities of China
Received date: 2017−07−25; **Accepted date:** 2017−11−20
Corresponding author: CHEN Ping, PhD, Associate Professor; Tel: +86–10–62332357; E-mail: chenp@ ustb.edu.cn

improve the load carrying capacity [7, 16].

Since the 1960s, a large number of processing techniques have been employed [4, 17–20], including electrical discharge texturing (EDT), reactive-ion etching (RIE), ion beam texturing, laser surface texturing (LST) and machining. For example, ZHOU et al [17] studied the influence of electrical discharge textures on the tribological behaviour of aluminum sheets. WANG et al [4] presented that the surface patterns fabricated using RIE enhanced the lift of seals by raising the additional hydrodynamic pressure. Their studies indicated that the optimum dimple geometry and distribution form at least doubled the load-carrying capacity relative to untextured surfaces. GRABON et al [18] studied experimentally the possibility of enhancing the tribological properties of honed cylinder liner surfaces by a burnishing technique. MENEZES et al [21] prepared surface patterns on the die surface by grinding and analyzed the influence of the surface pattern of the harder plate on coefficient of friction and formation of transfer layer under unlubricated and lubricated conditions. ZHANG et al [19] fabricated circle dimple textures using photolithography and electrolytic etching on the surface of 316 stainless steel and UHMWPE to comparatively investigate texture effects and their dependence on material, speed and load. The results showed that the tribo-pair with patterns on the UHMWPE side exhibited better wear resistant property than on the steel side. At present the most widely used technique is LST to fabricate different surface patterns on various material surfaces. OKSANEN et al [20] studied the influence of indirect LST and WS_2 addition on the tribological performance of Ta-C thin films at high temperatures. They found that the LST improved the wear life of WS_2/Ta–C surfaces by over 100% relative to a non-textured surface. CHEN et al [22] studied the influence of LST and surface coating on the tribological performance of stamping die steel, and found that both the triangle texture and TiN thin films presented good effectiveness in decreasing loss from friction and wear.

Different textures have been investigated in recent years and more specifically dimple patterns [4, 6, 19, 23]. WANG et al [23] investigated the dimple size effect on the friction and the load carrying capacity between cylindrical and plane surfaces. BIBOULET et al [24] experimentally studied a flat oil control ring and showed that a cross-hatched pattern improved its load-carrying capacity. Reports by YAN et al [25] also showed that a micro-circulation grid texture can dramatically decrease the coefficient of friction. Micro-groove textures are often characterized as lubricant pools and pipes redistributing lubricant and in addition can adjust the load-carrying capacity and pressure distribution. The work conducted by YIN et al [26] on lubrication performance of the micro-groove textured surface for diesel engine cylinder liners showed that the micro-groove could generate film pressure to provide lubrication between cylinder liner and piston ring. A report by XING et al [27] on lined grooved and wavy grooved textures fabricated on the surface of Si_3N_4/TiC ceramics showed that the wavy grooves presented the lowest frictional coefficient in unlubricated and MoS_2 solid lubricated conditions. YUAN et al [28] indicated that the micro-groove textures oriented slant to the sliding direction (neither parallel nor perpendicular to the direction of friction movement) made use of both parallel and perpendicular orientations under lubricated condition. In general, both parallel and perpendicular to the direction of friction movement are two special cases of micro-grooves direction. The influence of micro-grooves different from parallel and perpendicular to the direction of movement is anticipated to exist between these extreme cases. Moreover, the direction of micro-groove textures maybe strongly affects the tribological performance of friction surfaces in an unlubricated state. This paper addresses experimentally this problem focusing on the effect of geometric micro-groove texture patterns, and compares the tribological performance of micro-grooved texture surfaces and untextured surfaces in lubricated and unlubricated conditions, respectively.

2 Experiments

2.1 Specimens

The pins and disks for tribological tests were both made of 1Cr18Ni9Ti stainless steel. The hardness of the stainless steel selected is 279–306 HV measured by the Vickers micro-hardness tester with a load of 100 g and a dwell time of 10 s.

The pin specimens were in the form of cylinder, a height of 13 mm and a flat contact area

with a diameter of 8 mm. To remove the burrs that might have been formed during machining, all pin specimens were polished and cleaned with alcohol in an ultrasonic bath to reach a surface roughness of R_a 0.02 μm.

The disk specimens have a diameter of 24 mm and a thickness of 7.88 mm. To investigate the effect of geometric micro-groove texture patterns (Figure 1), disk specimens were fabricated with four kinds of micro-grooves using an MFT-20 laser processing system as well as a two-step LST process to remove the burrs inside the texture and make it smooth. The basic laser process parameters are listed in Table 1 and the pattern layouts are shown in Figure 1. Here, the area ratio of texture was designed as 0.05. Before the LST process, the disk specimens were polished using sandpapers to reduce surface roughness (R_a 0.1 μm). During the LST process, molten metal accumulated and became burrs around the edge of micro-grooves. The burrs might result in a high surface roughness and would influence the tribological performance of the tribo-pairs. Hence, the disk specimens were placed onto a polishing machine, running at 200 r/min, for 5 min. And the same polishing procedure was used for all disk specimens to ensure that differences between test results were due to geometric micro-groove texture patterns rather than surface roughness.

2.2 Procedures

Friction tests were conducted reciprocating sliding against a UMT-II pin-on-disk tribometer. Disks were fixed to the moving ground plate of the tribometer while upper pins were attached to the lever arm. A constant applied load of 1 N was carried out through a dead weight. The sliding speed of the test was controlled by changing the moving speed of the disk, and the sliding direction was described with a white bidirectional arrow shown in Figure 1. The disk was "running-in" for a 1 min period using a load of 1 N and a sliding speed of 0.05 m/s before commencing friction measurements. In this process, great care should be taken to ensure true flat-on-flat contact between the pin and the disk. The one-way sliding distance was

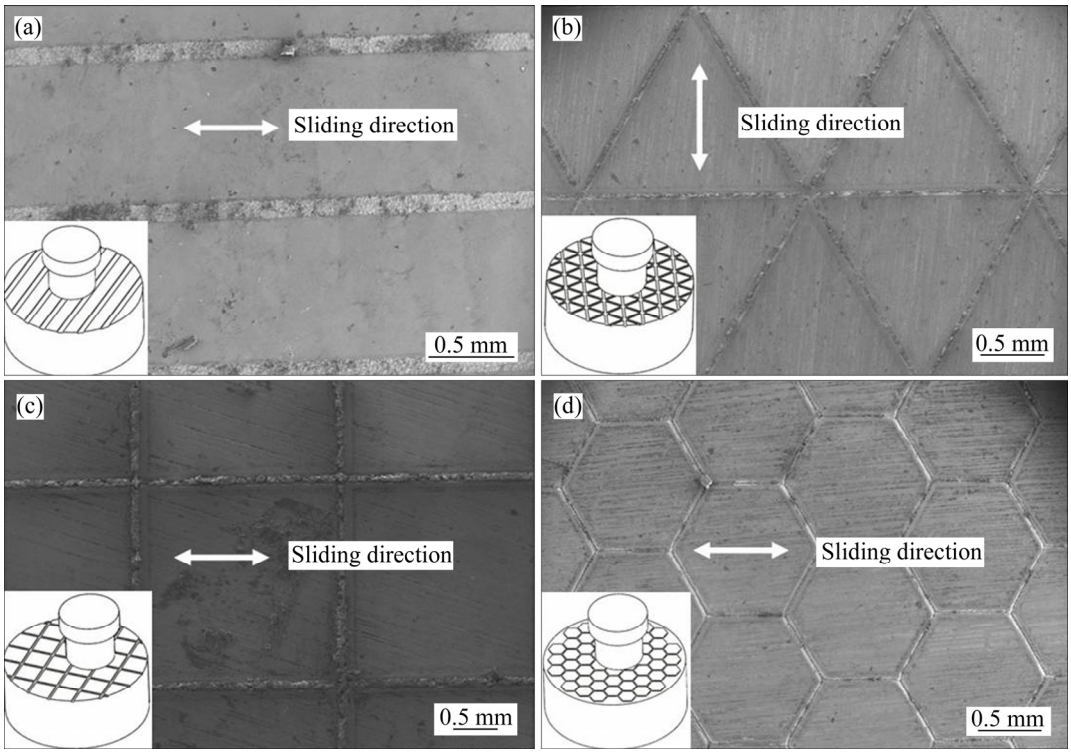

Figure 1 Geometric patterns of micro-grooves: (a) Parallel; (b) Triangular; (c) Square; (d) Hexagonal

Table 1 Parameters of laser micromachining system

Parameter	Max. output power/W	Pulse repetition rate/kHz	Emission wavelength/nm	Carving depth/mm	Carving linear speed/(mm·s^{-1})	Min. line width/mm	Repeatability precision/mm
Value	20	20–1000	1064	≤0.4 mm	≤ 7000	0.05	±0.003

5 mm. Ambient temperature and relative humidity (RH) were kept constant during all experiments (25 °C and 41% RH).

The first experiment measured the frictional coefficients of the micro-groove textured samples and the untextured ones (as a comparison) in a lubricated state. The disks were lubricated with SE 15W-40 oil. The viscosity of the oil at 25 °C was measured using a rotational rheometer and found to be 0.23 Pa·s. At the start of each test, two drops of lubricant (less than 4×10^{-3} mL/cm^2) were applied to the top surface of the disk. Tests were conducted at increasing sliding speeds ranging from 0.05 m/s to 2.5 m/s in steps of 0.05 m/s. The testing time at each speed was maintained for 1 min, that is, the testing time of each series was 50 min.

The second experiment used a new disk and repeated the friction measurement in an unlubricated state; this time the speed was a constant with a sliding speed of 0.6 m/s and a testing time of 3 h for each tribo-pair.

Both unlubricated and lubricated experiments were repeated twice using the same testing procedures. All measured data were analysed using MATLAB and the average values as well as the standard deviations were calculated.

For micro-grooves, the exact dimensions (depth and width) were assessed by means of three-dimension white light interferometry as well as by digital optical microscopy. Scanning electron microscopy (SEM) was also used to analyze the samples after the friction tests.

3 Results and discussion

3.1 Characterization of surface textures

Scanning electron microscopy images of four kinds of micro-groove textured surfaces making parallel, triangular, square and hexagonal patterns are presented in Figure 1. It can be seen that the parallel pattern has a texture pitch of 1 mm (Figure 1(a)); the isometric triangle pattern has a micro-groove length of 1.73 mm (Figure 1(b)); the isometric square pattern has a micro-groove length of 0.92 mm (Figure 1(c)) and the isometric hexagon pattern has a micro-groove length of 0.56 mm (Figure 1(d)).

Three-dimensional and two-dimensional optical profilometry images of micro-grooves are presented in Figures 2 and 3. The images show that the two-step LST process and burr removal process were conducted successfully. The surface roughness (R_a) of the sample is around 0.15 μm. The samples were extremely uniform and featured micro-grooves of precise geometrical parameters. The average width of the micro-grooves is 52–53 μm and the average depth is around 22 μm.

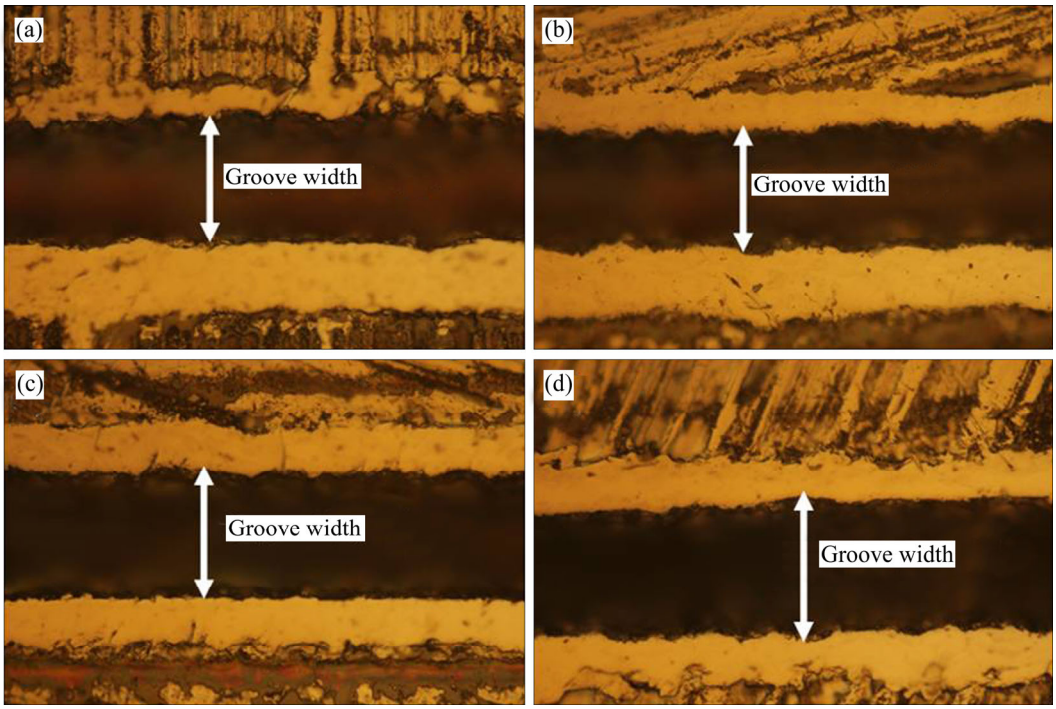

Figure 2 2D optical profilometry images of micro-grooves: (a) Parallel; (b) Triangular; (c) Square; (d) Hexagonal

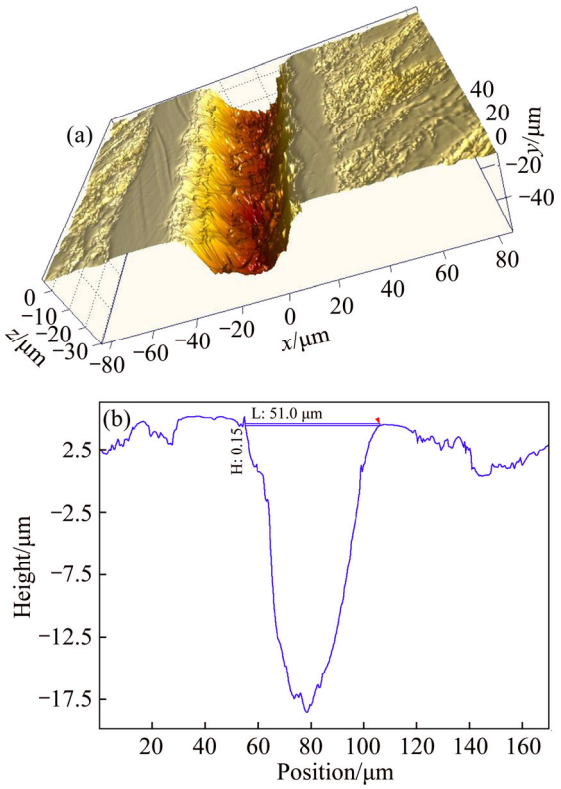

Figure 3 Optical profilometry images of a micro-groove: (a) 3D surface morphology; (b) 2D cross profile

3.2 Tribological performance

3.2.1 Lubricated test results

Under lubricated conditions, starting from the lowest speed (0.05 m/s), the speed was increased gradually after 1 min at each sliding speed, until the highest speed of 2.5 m/s was reached. The whole testing time was 3000 s. Figure 4 exhibits the coefficient of friction curves of the relationship between the frictional coefficient and the testing time. It can be observed that the surface texture influenced the fluctuation of frictional coefficient in the lubricated state. The frictional coefficients of the untextured samples fluctuated wildly and frequently whereas the micro-groove textured samples showed much less fluctuation. Frictional coefficients started rising after 700–800 s of testing; for the square-patterned sample, the frictional coefficient was notably more stable than other results.

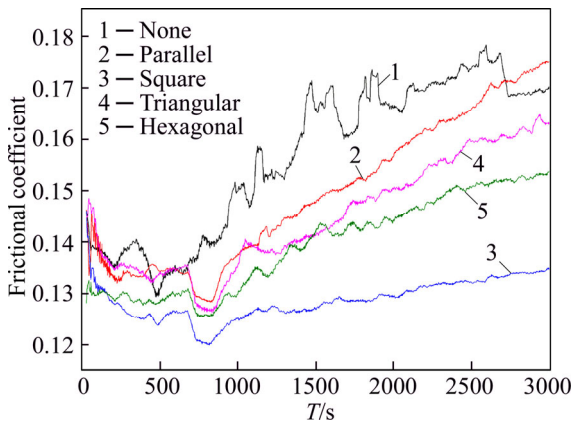

Figure 4 Frictional coefficient curves under lubricated conditions (sliding speed range of 0.05–2.5 m/s)

Figure 5 presents the average frictional coefficient of samples at each sliding speed. From the experimental data in Figure 5, it can be found that the average frictional coefficients of untextured samples were larger than those of micro-groove textured samples at different speeds except for the sliding speed of 0.05 m/s and above the sliding speed of 2.05 m/s. All frictional coefficient curves show a minimum occurring in the sliding speed ranging from 0.1 m/s to 0.7 m/s; the effect is more pronounced for the square textured surface which is closer to maintaining a relatively stable frictional coefficient over the entire speed range. At the sliding speed of 0.05 m/s, the frictional coefficient of the untextured sample (0.141) was lower than that of the triangular micro-groove textured sample (0.147). As well as at the speed range of 2.05–2.5 m/s, the frictional coefficients of untextured sample were lower than those of parallel micro-groove textured samples. The experimental data also show that the frictional coefficient of untextured samples changed irregularly with increasing of speed, and the lowest frictional coefficient (0.13) was achieved at the speed of 0.4 m/s. However, there is a very similar trend almost for all micro-groove textured samples. When the speed was less than 0.4 m/s, the frictional coefficients continuously decreased with increasing sliding speed, and followed by a sudden increase slightly at the sliding speed of 0.45 m/s. When the sliding speed was 0.55 m/s, the frictional coefficient reached the minimum value (0.12, 0.125, 0.127 and 0.129 for square, hexagonal, triangular and parallel micro-groove textures, respectively). Then the frictional coefficient increased linearly with increasing of sliding speed. Compared with all geometric micro-groove texture patterns, square micro-grooves achieved the lowest frictional coefficient, followed by hexagonal, triangular and parallel micro-grooves, respectively. And with the increase of sliding speed, the increasing rates of frictional coefficients were different when the speed

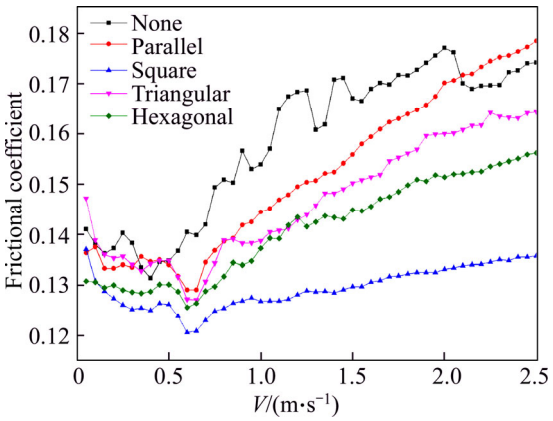

Figure 5 Average frictional coefficients at each speed under lubricated conditions

was above 0.55 m/s. Square micro-grooves had the slowest increasing rate, and parallel micro-grooves had the fast one. As the sliding speed increased to 2.5 m/s, the frictional coefficients of square, hexagonal, triangular and parallel micro-groove samples are 0.136, 0.156, 0.164 and 0.178, respectively.

There may be some reasons responsible for the above results. The micro-groove textured surfaces not only act as a reservoir to capture abrasive or liquid lubricant replenishment, but also produce a good hydrodynamic effect between the sliding surfaces as compared with the untextured surfaces, and the lubricant stored in the micro-grooves can increase the film thickness and film carrying capacity to reduce the friction [29], which is one possible reason to explain why the frictional coefficients of the untextured samples are higher than those of micro-groove textured samples as shown in Figure 5. The experimental data of micro-groove textured samples obtained from different sliding speeds could not present a typical Stribeck curve during the whole test. That might be because the oil lubricant was limited (two drops at the start of each test) and the wear occurred when the sliding speed increased. The results are also similar to the well accepted conclusion reported by WANG et al [23] that the fluid dynamic pressure effect would become not significant at low-load and high-speed condition. In addition, differences also exist between the Stribeck curves due to the different applied loads, the applied load was lower and constant in the present test which differs significant with that in Refs. [15, 30] where the applied loads were heavy and varied.

The experimental data from Figures 4 and 5 also manifested that the micro-groove textures perpendicular or parallel to the direction of movement had a obvious influence on the tribological properties of tribo-pairs. For the purpose of easy understanding, the analysis results are illustrated by Figure 6. To analyze the occurrence of the lowest frictional coefficient phenomenon for the square micro-groove samples, the pattern of a square micro-groove can be decomposed into two directions according to the sliding direction (Figure 6(c)): ⊥orientation groove textures (oriented perpendicular to the direction of movement) and //orientation groove textures (oriented along the direction of movement). Compared with the hexagonal micro-groove textured samples, the frictional coefficient of the square micro-groove textured samples fluctuated obviously when the pin sample was sliding from one ⊥orientation groove to another within the testing time of 30 s (Figure 4). The reason suggested here probably was that the lack of lubricant increased the solid contact area and resulted in the slight deformation in the initial of the experiment. With increasing of testing time, the //orientation grooves provide oil supply to restrict solid contact area growth, and the ⊥orientation grooves may interrupt the slight deformation to reduce the fluctuation and achieve a lower frictional coefficient [10]. Moreover, the ⊥orientation grooves can be helpful for the formation of hydrodynamic pressure lubrication, and the liquid lubricant in the //orientation grooves will flow readily under the shear stress imposed by the above sample, to supply the liquid lubricant into the ⊥orientation grooves, and the result was to further enhance the effect of hydrodynamic pressure lubrication as well as improve the lubrication regime and reduce the frictional coefficient. The square micro-groove texture takes the merits of ⊥orientation grooves and //orientation grooves to generate the best influence on friction at most cases [28]. The result is consistent with the conclusion reported by YU et al [31] that the strongest hydrodynamic effect was obtained when the long axis of the texture was perpendicular to the direction of movement. For the pattern of a triangular micro-groove (Figure 6(b)), there are two ∠orientation grooves (oriented slant to the sliding direction), which may result in the tribological

performance of triangular micro-groove texture being worse than that of the square micro-groove texture. For the pattern of a hexagonal micro-groove (Figure 6(d)), the friction coefficient of hexagonal textures is lower than that of the parallel and triangular textures, and higher than that of the square textures. For the former, it results in the synergistic effect of parallel and triangular textures. Compared with the triangular textures, the // orientation grooves of the hexagonal textures can supply oil and restrict solid contact area growth. And compared with the parallel textures, the lubricant oil from the // orientation grooves flows to the ∠orientation grooves, not directly flow out. For the later, compared with the square textures, there is no ⊥orientation grooves of the hexagonal textures, which can produce the higher hydrodynamic pressure than that of the ∠orientation grooves. Based on the above orientation grooves analysis, it can be understood that the tribological performance of hexagonal micro-groove texture is between the square micro-groove texture and the triangular micro-groove texture. For the parallel micro-groove texture (Figure 6(a)), the grooves oriented along the sliding direction made the liquid lubricant flow out more likely, especially at higher sliding speed.

3.2.2 Unlubricated test results

Figure 7 shows the relationship between the frictional coefficient of samples and testing time at the speed of 0.6 m/s under unlubricated conditions. The frictional coefficients of all samples showed a higher fluctuation level in an unlubricated state (Figure 7) than that in a lubricated state (Figure 4). The experimental data in Figure 7 indicate that the frictional coefficients of micro-groove samples are lower than that of the untextured sample at the beginning of the experiment, and then the frictional coefficient increases by more than a factor of 1.6 (from 0.13 to 0.25) for the micro-groove textured samples, and the same for the untextured sample from 0.23 to 0.37. Figure 7 also indicates that the frictional coefficients of the untextured sample fluctuated significantly at the beginning of the test. This phenomenon may be resulted from the very top of the highest asperities of untextured surface contacted in the contact surface. And the micro-groove textured surface can not only trap wear debris but also reduce the contact area, thus reduce the friction of the two contact surfaces, which is more obvious in the low applied load [20]. It has also been reported that the roughness in the range 0.1 and 0.6 μm may not significantly change the frictional coefficient [11]. At the end of experiment process, the untextured samples made a larger noise than the micro-groove textured samples, especially than the parallel and hexagonal textures. This is probably due to the abrasives and particles originating from the contact surface under the dry friction conditions becoming squeezed between the surfaces.

The average frictional coefficients of all samples during the whole testing process are figured out as displayed in Figure 8. It can be observed that the average frictional coefficient of the untextured sample is 0.382, while the parallel texture sample and the hexagonal texture sample are 0.327 and 0.353, respectively, nearly 8 % lower

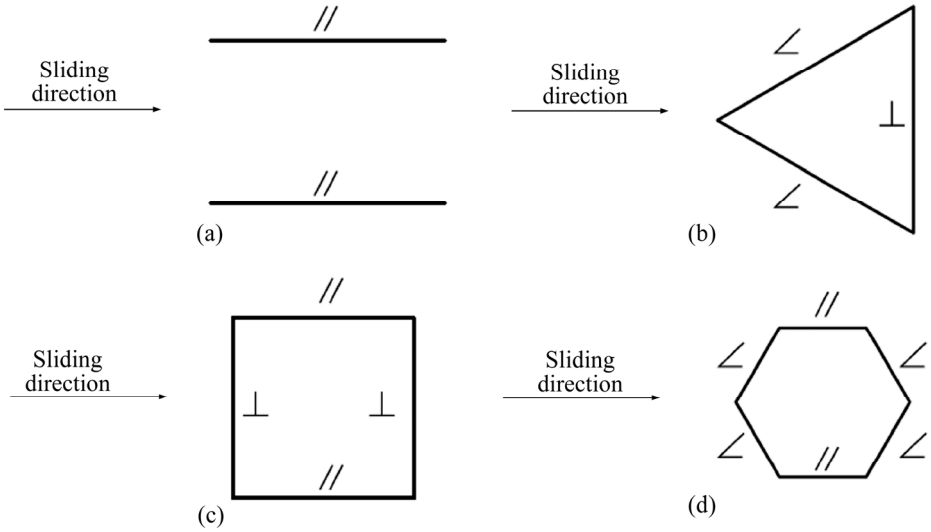

Figure 6 Groove orientation to sliding direction: (a) Parallel; (b) Triangular; (c) Square; (d) Hexagonal

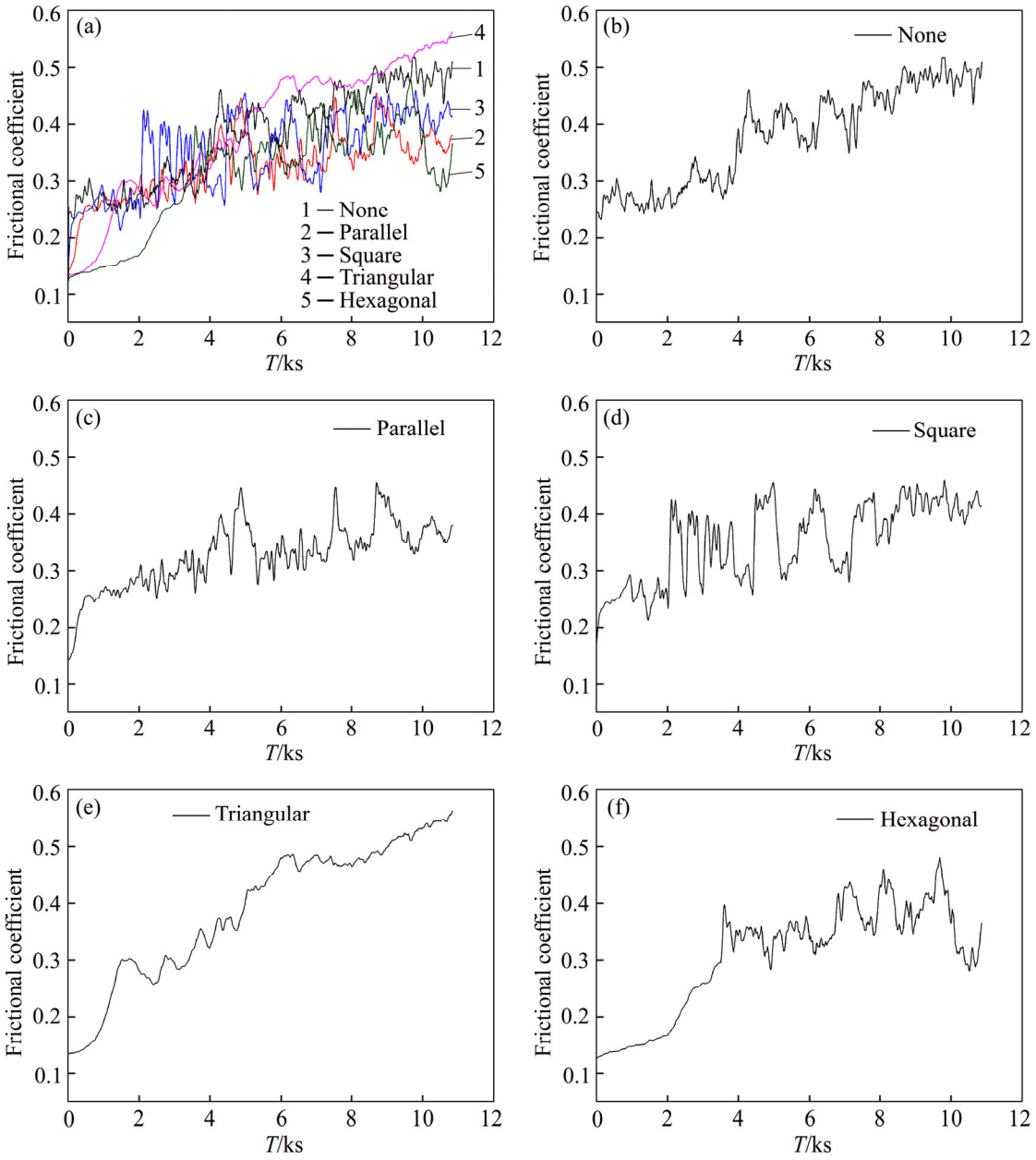

Figure 7 Frictional coefficient curves under dry friction conditions (sliding speed of 0.6 m/s)

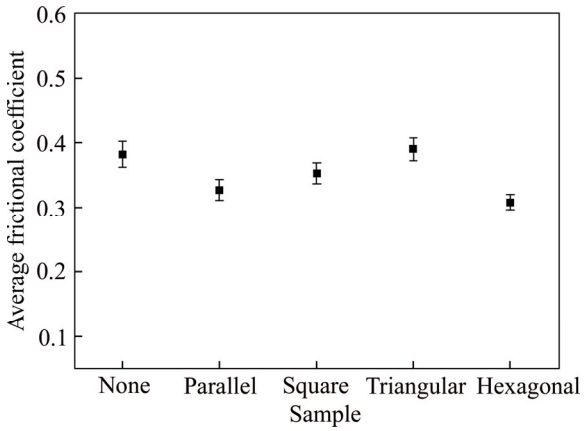

Figure 8 Average frictional coefficients under dry friction conditions (testing time of 3 h)

than that of the untextured sample due to the existence of micro-groove texture.

SEM images of worn surfaces for the textured and untextured samples are shown in Figure 1 and Figure 9. Some abrasives generated during the dry friction process can be seen both on the surface and in the grooves. Generally, under dry friction conditions, the abrasives on the surface form the "three-body friction" easily which will increase the frictional coefficient and induce the wear tracks, and the micro-grooves on the textured surface can not only capture abrasive but also reduce the effective contact area. Hence, it is obvious that

there are much more abrasives on the untextured surfaces (Figure 9(a)) than on the textured surfaces (Figure 1), which resulted in the high frictional coefficients and serious wear tracks for untextured samples (Figure 9(b)). In comparison with all micro-groove textured samples, the hexagonal textured sample has the lowest average frictional coefficients, followed by the parallel and square textured samples, while the triangular micro-groove textured sample has the highest frictional coefficient (0.39), slightly higher than that of untextured samples (0.38). These phenomena were probably illustrated by Figure 6. For the hexagonal micro-grooves, it has ∠orientation and // orientation grooves (Figure 6(d)). Hence, the ∠orientation grooves can capture abrasive, and // orientation grooves and the obtuse angle of the two adjacent grooves probably resulted in abrasive remove easily and timely. For the parallel grooves, there are only // orientation grooves along to the sliding direction (Figure 6(a)), no other orientation grooves to capture much more abrasives. For the triangular micro-grooves however, there is no // orientation grooves and the angle of the two adjacent grooves is acute (Figure 6(d)), which may be helpful to explain the higher frictional coefficients.

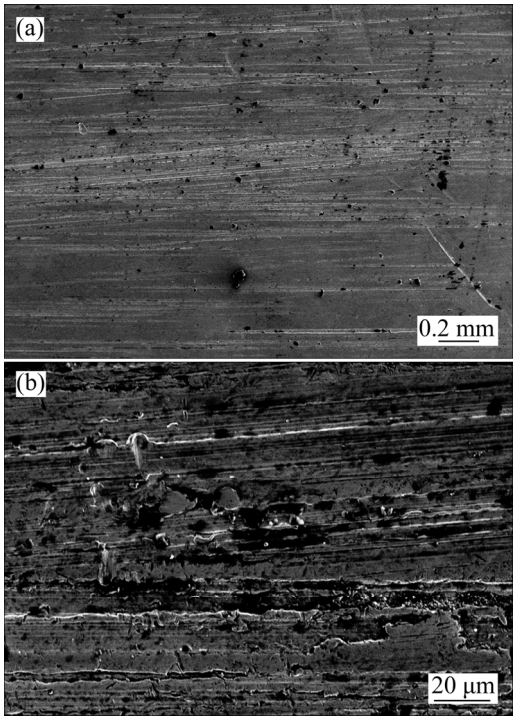

Figure 9 SEM images of untextured samples under dry friction conditions

4 Conclusions

A two-step laser surface texturing process was used to fabricate micro-groove textures. And a pin-on-disk tribometer was conducted to measure the tribological performance of the textured and untextured samples in lubricated and unlubricated state, respectively. The following summarizes the conclusions.

1) The high-precision micro-groove texture can be fabricated using the two-step LST process. The micro-groove texture friction pairs have lower coefficient of friction than the ones without textures and the geometric patterns have a significant influence on the tribological properties under both lubricated and unlubricated conditions.

2) Under lubricated conditions, the square micro-groove textured samples achieved the lowest frictional coefficients, followed by the hexagonal and triangular ones, which can be explained from the aspects of lubricant supply and hydrodynamic pressure. The direction of movement should therefore be taken into account when designing textured surfaces.

3) Under dry friction conditions, of the textured samples, the parallel and hexangular textured samples were the best at friction reduction, which can be explained from the aspects of abrasive trap and remove. As for the frictional coefficient of the triangular pattern higher than that of untextured sample, experiments and mechanism should be further studied.

Acknowledgement

The authors would like to express special thanks to SHAO Tian-min (State Key Laboratory of Tribology, Tsinghua University) for scientific guidance and Petre Denissenko and Roger Moss (The University of Warwick) for English writing assistance.

References

[1] GHIOTTI A, BRUSCHI S, MEDEA F. A hamasaiid tribological behavior of high thermal conductivity steels for hot stamping tools [J]. Tribology International, 2016, 97: 412–422.

[2] SHAO Tian-min, GENG Zhe, Research progress in patterned

thin solid film techniques and their tribological performance [J]. China Surface Engineering, 2015, 28: 1–26. (in Chinese)

[3] MAGDALENA N W, WITOLD P. The surface texture and its influence on the tribological characteristics of a friction pair: Metal-polymer [J]. Archives of Civil and Mechanical Engineering, 2017, 17(2): 344–353.

[4] WANG Xiao-lei, KATO K. Improving the anti-seizure ability of SiC seal in water with RIE texturing [J]. Tribology Letters, 2003, 14: 275–280.

[5] ETSION I. State of the art in laser surface texturing [J]. Journal of Tribology, 2005, 17: 761–762.

[6] WU Ze, XING You-qiang, HUANG Peng, LIU Lei. Tribological properties of dimple-textured titanium alloys under dry sliding contact [J]. Surface Coating & Technology, 2017, 309: 21–28.

[7] HAMILTON D B, WALOWIT J A, ALLEN C M. A theory of lubrication by microirregularities [J]. Journal of Basic Engineering, 1966, 86: 177–185.

[8] ETSION I, BURSTEIN L. A model for mechanical seals with regular microsurface structure [J]. Tribology Transaction, 1996, 39: 677–683.

[9] QIU Ming-feng, DELLIC A, RAEYMAEKER B. The effect of texture shape on the load-carrying capacity of gas-lubricated parallel slider bearings [J]. Tribology Letters, 2012, 48(3): 315–327.

[10] PETTERSSON U, JACOBSON S. Friction and wear properties of micro textured DLC coated surfaces in boundary lubricated sliding [J]. Tribology Letters, 2004, 17: 553–559.

[11] SCHUH J K, EWOLDT R H. Asymmetric surface textures decrease friction with Newtonian fluids in full film lubricated sliding contact [J]. Tribology International, 2016, 97: 490–498.

[12] LING T D, LIU Pin-zhi, XIONG Shang-wu, GRZINA D, CAO Jian, WANG Q J, XIA Z C, TALWAR R. Surface texturing of drill bits for adhesion reduction and tool life enhancement [J]. Tribology Letters, 2013, 52: 113–122.

[13] KOVALCHENKO A, AJAYI O, ERDEMIC A, FENSKE G. Friction and wear behavior of laser textured surface under lubricated initial point contact [J]. Wear, 2011, 271: 1719–1725.

[14] RYK G, KLIGERMAN Y, ETSION I. Experimental investigation of laser surface texturing for reciprocating automotive components [J]. Tribology Transaction, 2002, 45: 444–449.

[15] BORGHI A, GUALTIERI E, MARCHETTO D, MORETTI L, VALERI S. Tribological effects of surface texturing on nitriding steel for high-performance engine applications [J]. Wear, 2008, 265: 1046–1051.

[16] MOHAMMAD T, MUCHAMMAD J. Numerical study of the load-carrying capacity of lubricated parallel sliding textured surfaces including wall slip [J]. Tribology Transaction, 2014, 57: 134–145.

[17] ZHOU Rui, CAO Jian, WANG Q J, MENG Fan-ming, ZIMOWKSI K, XIA Z C. Effect of EDT surface texturing on tribological behavior of aluminum sheet [J]. Journal of Materials Processing Technology, 2011, 211: 1643–1649.

[18] GRABON W, KOAZELA W, PAWLUS P, OCHWAT S. Improving tribological behaviour of piston ring-cylinder liner frictional pair by liner surface texturing [J]. Tribology International, 2013, 61: 102–108.

[19] ZHANG Bo, WANG Hui, WANG Jing-qiu, WANG Xiao-lei. Comparison of the effects of surface texture on the surfaces of steel and UHMWPE [J]. Tribology International, 2013, 65: 138–145.

[20] OKSANEN J, HAKALA T J, TERVAKANGAS S, LAAKSO P, KILPI L, RONKAINEN H, KOSKINEN J. Tribological properties of laser-textured and ta-C coated surfaces with burnished WS_2 at elevated temperatures [J]. Tribology International, 2014, 70: 94–103.

[21] MENEZES P L, KISHORE, S V KAILAS M R LOVELL. The role of surface texture on friction and transfer layer formation during repeated sliding of Al-4Mg against steel [J]. Wear, 2011, 271: 1785–1793.

[22] CHEN Ping, XIANG Xin, SHAO Tian-min, LA Ying-qian, LI Jun-ling. Effect of triangular texture on the tribological performance of die steel with TiN coatings under lubricated sliding condition [J]. Applied Surface Science, 2016, 389: 361–368.

[23] WANG Xiao-lei, LIU Wei, ZHOU Fei, ZHU Di. Preliminary investigation of the effect of dimple size on friction in line contacts [J]. Tribology International, 2009, 42: 1118–1123.

[24] BIBOULET N, BOUASSIDA H, LUBRECHT A A. Cross hatched texture influence on the load carrying capacity of oil control rings [J]. Tribology International, 2015, 82: 12–19.

[25] YAN L U, LIU Zuo-ming. Lubrication performance of the grid-patterned microcirculation surface [J]. Tribology, 2013, 33: 357–362. (in Chinese)

[26] YIN Bi-feng, QIAN Yan-qiang, LI Xiao-dong, LIU Sheng-ji, FU Yong-hong. Simulation and analysis on lubrication performance of surface micro-groove texturing on cylinder liner in diesel engine [J]. China Mechanical Engineering, 2013, 24: 644–650. (in Chinese)

[27] XING You-qiang, DENG Jian-xin, WU Ze, CHENG Hong-wei. Effect of regular surface textures generated by laser on tribological behavior of Si_3N_4/TiC ceramic [J]. Applied Surface Science, 2013, 265: 823–832.

[28] YUAN Si-huan, HUANG Wei, WANG Xiao-lei. Orientation effects of micro-grooves on sliding surfaces [J]. Tribology International, 2011, 44(9): 1047–1054.

[29] CHOUQUET C, GAVILLET J, DUCROS C, SANCHETTE F. Effect of DLC surface texturing on friction and wear during lubricating sliding [J]. Materials Chemical Physics, 2010, 123: 367–371.

[30] BEOMKEUN K, YOUNG H C, HEUNG S C. Effects of surface texturing on the friction behavior of cast iron surfaces [J]. Tribology International, 2014, 70: 128–135.

[31] YU Hai-wu, WANG Xiao-lei, ZHOU Fei. Geometric shape effects of surface texture on the generation of hydrodynamic pressure between conformal contacting surfaces [J]. Tribology Letters, 2010, 37: 123–130.

(Edited by HE Yun-bin)

中文导读

微凹槽织构几何分布对不锈钢摩擦学性能的影响

摘要：本文实验研究了表面织构沟槽的几何分布对不锈钢摩擦学性影响。沟槽的分布形式分别是平行、三角形、正方形和六边形，并对比研究无织构形式。利用 MFT-20 激光系统加工织构，采用销-盘磨损试验机测试其摩擦学性能，同时利用扫描电镜观察分析微观形貌。结果表明，先粗加工后精加工的方法可加工出高精度织构；有织构试样的摩擦系数低于无织构的摩擦系数，且织构的几何分布影响润滑状态和无润滑状态下试样的摩擦学性能。从润滑油的供给和流体动压润滑效应分析了润滑状态下的摩擦磨损机理；从磨屑的捕捉以及去除分析了无润滑状态下的摩擦磨损机理。

关键词：几何分布；微凹槽织构；摩擦系数